RADIATION RESEARCH **190**, 164–175 (2018)
0033-7587/18 $15.00

DOI: 10.1667/RR14993.1

Selective Insulin-like Growth Factor Resistance Associated with Heart Hemorrhages and Poor Prognosis in a Novel Preclinical Model of the Hematopoietic Acute Radiation Syndrome

Doreswamy Kenchegowda,[a] Betre Legesse,[a] Bernadette Hritzo,[a] Cara Olsen,[b] Saeed Aghdam,[a] Amandeep Kaur,[a] William Culp,[c] Alexandrine Derrien-Colemyn,[a] Grant Severson[a] and Maria Moroni[a,1]

[a] *Scientific Research Department, Armed Forces Radiobiology Research Institute, Bethesda, Maryland; and* [b] *Biostatistics Consulting Center and* [c] *Office of the Vice President for Research, Uniformed Services University of the Health Sciences, Bethesda, Maryland*

Kenchegowda, D., Legesse, B., Hritzo, B., Olsen, C., Aghdam, S., Kaur, A., Culp, W., Derrien-Colemyn, A., Severson, G. and Moroni, M. Selective Insulin-like Growth Factor Resistance Associated with Heart Hemorrhages and Poor Prognosis in a Novel Preclinical Model of the Hematopoietic Acute Radiation Syndrome. *Radiat. Res.* 190, 164–175 (2018).

Although bone marrow aplasia has been considered for the past decades as the major contributor of radiation-induced blood disorders, cytopenias alone are insufficient to explain differences in the prevalence of bleeding. In this study, the minipig was used as a novel preclinical model of hematopoietic acute radiation syndrome to assess if factors other than platelet counts correlated with bleeding and survival. We sought to determine whether radiation affected the insulin-like growth factor-1 (IGF-1) pathway, a growth hormone with cardiovascular and radioprotective features. Gottingen and Sinclair minipigs were exposed to ionizing radiation at hematopoietic doses. The smaller Gottingen minipig strain was more sensitive to radiation; differences in IGF-1 levels were minimal, suggesting that increased sensitivity could depend on weak response to the hormone. Radiation caused IGF-1 selective resistance by inhibiting the anti-inflammatory anti-oxidative stress IRS/PI3K/Akt but not the pro-inflammatory MAPK kinase pathway, shifting IGF-1 signaling towards a pro-oxidant, pro-inflammatory environment. Selective IGF-1 resistance associated with hemorrhages in the heart, poor prognosis, increase in C-reactive protein and NADPH oxidase 2, uncoupling of endothelial nitric oxide synthase, inhibition of nitric oxide (NO) synthesis and imbalance between the vasodilator NO and the vasoconstrictor endothelin-1 molecules. Selective IGF-1 resistance is a novel mechanism of radiation injury, associated with a vicious cycle amplifying reactive oxygen species-induced damage, inflammation and endothelial dysfunction. In the presence of thrombocytopenia, selective inhibition of IGF-1 cardioprotective function may contribute to the development of hemostatic disorders. This finding may be particularly relevant for individuals with low IGF-1 activity, such as the elderly or those with cardiometabolic dysfunctions.

Editor's note. The online version of this article (DOI: 10.1667/RR14993.1) contains supplementary information that is available to all authorized users.

[1] Address for correspondence: Armed Forces Radiobiology Research Institute, Building 42, 8901 Wisconsin Ave., Bethesda, MD 20889; email: maria.moroni@usuhs.edu.

INTRODUCTION

The Gottingen minipig (GMP) has a higher sensitivity to acute ionizing radiation than other species (*1*) and minipig breeds (*2, 3*). Acute radiation syndrome (ARS) in GMP is characterized by widespread edema and hemorrhages at relatively low doses, affecting mainly heart, lung, brain and intestine (*4*). In the GMP model, damage to vasculature is considered to be one of the main determinants of radiosensitivity.

The Gottingen minipig is one of the smallest among the miniature swine breeds available for research. The small size of the GMP has been attributed to pituitary dwarfism and deficiency in growth hormones (GH, IGF-1), since miniature swine have generally lower levels of growth hormones compared to conventional breeds (*5*). The insulin-like growth factor-1 (IGF-1) is a hormone produced primarily by the liver in response to the growth hormone (GH). It is structurally similar to insulin, with which it shares several intracellular signaling mediators and pathways (*6, 7*). IGF-1 displays pleiotropic functions including regulation of growth, lipid and carbohydrate metabolism, apoptosis, oxidative stress and vascular homeostasis in the heart (*8, 9*). Environmental stressors that affect the regulation of the insulin/IGF-1 system are therefore likely to induce severe cardiovascular damage.

Among the most important cardiovascular functions of IGF-1 is the regulation of vascular tone through two major, distinct pathways: the anti-inflammatory/anti-oxidative stress PI3K/Akt pathway and the pro-inflammatory Grb/Shc/MAPK (PI3K/Akt independent) pathway [reviewed in

(*10*)]. Activation of the IRS/PI3K/Akt leads to the phosphorylation of eNOS at Ser1179 and increase in the production of nitric oxide (NO) within minutes. Nitric oxide is a powerful vasodilator with anti-thrombotic and anti-inflammatory properties. eNOS produces NO from the conversion of L-arginine to L-citrulline, in the presence of tetrahydrobiopterin (BH4). In the absence of BH4, eNOS becomes uncoupled and catalyzes the formation of superoxide instead of NO (*11*). Alteration in the bioavailability of NO is the determinant of endothelial dysfunction, a pathology associated with a variety of cardiovascular diseases and the onset of pro-thrombotic and pro-inflammatory vascular features (*7*). Interestingly, in cases of endothelial dysfunction, NO is decreased, although eNOS expression is often found to be increased (*12, 13*).

The Grb/Shc/MAPK pathway is used by IGF-1 to stimulate the expression of endothelin-1 (ET-1). ET-1 is a vasoconstrictor molecule with pro-inflammatory roles that antagonizes the function of NO (*7, 14*). Selective inhibition of IRS/PI3K/Akt/eNOS-dependent signaling in the presence of an active Grb/Shc/MAPK/ET pathway causes an imbalance between the production of NO and ET-1, leading to endothelial dysfunction and vascular diseases (*10*). Selective insulin/IGF-1 resistance has been shown to affect a variety of tissues including heart, kidney and liver (*10*). An example of the effect of insulin/IGF-1 selective inhibition is represented by cardiovascular complications among diabetic patients. In the arteries of these individuals, the anti-atherogenic properties of the PI3K/Akt pathway are lost, whereas activation of the MAPK/ET-1 pathway promotes pro-atherogenic signaling, eventually causing development of atherosclerosis (*7, 10*).

C-reactive protein (CRP) and renin-angiotensin system (RAS) are among the negative regulators of IGF-1 vascular-protective features. CRP is induced by oxidative stress, and promotes endothelial dysfunction both *in vitro* and *in vivo* through degradation of vascular protective layers, induction of NO deficiency, blunting of Akt activation, uncoupling eNOS and generation of superoxide (*15–20*). In children and adults, elevated CRP levels are associated with impaired vasoreactivity and reduced NO bioavailability (*21, 22*). Angiotensin activates redox-sensitive pathways, including MAPK, and stimulates the production of oxidative stress through NADPH oxidase (*23*). Increase in superoxide can promote the inhibition of PI3/Akt pathway and decrease NO bioavailability while inducing ET-1. In the absence of proper regulatory mechanisms, the overall outcome is a shift towards vasoconstriction, decreased blood flow, hypoperfusion and further generation of oxidative stress resulting in a self-feeding pattern of vascular dysfunction, inflammation and thrombosis.

Emerging evidence in clinical and laboratory settings indicates a role for IGF-1 in response to radiation. After irradiation, IGF-1 and its receptors (IGF-1R) are induced, and act as a radioprotectant by displaying protection against apoptosis, DNA damage and oxidative stress (*24*). In clinical settings, inhibition of IGF-1 has been proposed for potentiating the effect of radiotherapy on cancer cells (*24*). In the laboratory settings, administration of IGF-1 has been shown to increase survival, ameliorate organ function at both hematopoietic and gastrointestinal radiation doses, stimulate crypt expansion and regeneration (*25–30*), mitigate bone marrow toxicity, protect hematopoietic stem and progenitor cells from apoptosis and stimulate proliferation and differentiation of the surviving hematopoietic progenitor (*25–30*). Furthermore, in animal models receiving IGF-1, vascular superoxide levels have been shown to decrease, while NO bioavailability increased (*31*). In terms of late effects, the IGF-1 pathway was found to be inactivated in cardiovascular endothelial cells isolated from mice 16 weeks postirradiation with 8 or 16 Gy. This finding potentially links IGF-1 to radiation-induced cardiovascular dysfunction (*32*). In the past several years, we have developed GMP as an alternative large animal model for radiation countermeasure testing. We characterized the hematopoietic and gastrointestinal-ARS and established translational potential of the model (*1, 4, 33–35*). To further advance the development of animal models for radiation countermeasure testing under the FDA Animal Rule, the mechanisms of radiation injury and the differential radiation sensitivity among animal models need to be understood. Several published studies have indicated that hemorrhagic disorders may be caused by coagulopathies other than low platelet counts, for example, abnormal platelet or vascular function and inflammation (*36*). IGF-1 has a major role in maintaining vascular integrity, counteracting inflammation and providing a protective action against radiation. The small size of the GMP and its propensity to develop vascular damage and hemorrhage after irradiation, prompted us to investigate the association between IGF-1 and radiation injury. Furthermore, we assessed how radiation modulated IGF-1 signaling in the GMP, particularly in the context of the regulation of vascular tone and endothelial dysfunction.

MATERIALS AND METHODS

Animal Care and Irradiation

Male 3-to-5-month-old Gottingen minipigs (GMP; n = 48), weighing 8–12 kg, and Sinclair minipigs (SMP; n = 24), weighing 10–14 kg, were purchased from Marshall BioResources (North Rose, NY) and Sinclair BioResources (Columbia, MO), respectively. During the study period, minipigs were housed in the Veterinary Science Department, Armed Forces Radiobiological Research Institute (AFRRI, Bethesda, MD). All procedures performed in this study were in accordance with protocols approved by AFRRI's Institutional Animal Care and Use Committee (IACUC) and the Guide for the Care and Use of Laboratory Animals. Throughout the study, animals were maintained on a 12 h light–dark schedule and were provided with species-appropriate environmental enrichment. Animal rooms were maintained at 61–81°F and 30–70% relative humidity. Minipigs were singly housed to allow individual assessment of feed consumption and fecal/urine/blood production. Although singly housed, visual, olfac-

TABLE 1
Survival Rate Monitored of Gottingen and Sinclair Minipig for 45 Days Postirradiation (0.6 Gy/min TBI using ^{60}Co Gamma Photons)

Dose (Gy)	Gottingen (n = 12/dose)	Sinclair (n = 4–6/dose)
1.7	100%	Not determined
1.8	Not determined	100%
1.9	75%	Not determined
2.1	50%	100%
2.3*	25%	100%

* $P = 0.024$ (log-rank analysis).

tory and auditory contact with other minipigs was allowed to support their highly social nature. Animals were acclimatized for two weeks, provided with pig chow twice daily as per animal vendor recommendations and given free access to water.

Irradiation of minipigs was performed as described elsewhere (*4*). Briefly, animals were anesthetized by single intramuscular injection of a mixture of Telazol® (2 mg/kg) and xylazine (1 mg/kg), and received total-body irradiation (TBI) using cobalt-60 (^{60}Co) gamma photons (0.6 Gy/min). Dose rates in phantoms of various diameters are characterized annually at AFRRI using alanine dosimetry system against two national standard laboratories. Real-time dosimetry was performed for each irradiation with an ionization chamber located in the radiation field, but not in the path of the radiation beam directed toward the animal. Radiation doses ranged from 1.7–2.3 Gy (Table 1) and the day of exposure was considered ''day 0''. The animals were followed for 45 days postirradiation and were provided minimum preventive supportive care throughout the course of the study. Moribund animals were euthanized when they showed at least one symptom from absolute criteria (nonresponsiveness, dyspnea, hypothermia) or a combination of four nonabsolute criteria [hypothermia, anorexia, anemia, vomiting/diarrhea, lethargy, vestibular signs and prolonged hemorrhage (*4*)]. Animals that survived the entire study period were considered as survivors, however, the animals euthanized due to radiation-induced illness were considered decedents. For further comparisons, animals were grouped into survivors and decedents regardless of the radiation doses.

Blood and Tissue Collection

Blood samples were collected longitudinally from saphenous or cephalic vein under isoflurane anesthesia at days –7, –1, +1, +3, +7 and twice weekly thereafter. Samples were collected in EDTA tubes and immediately processed for complete blood counts with differentials using the ADVIA 2120 (Siemens Medical Solutions Diagnostics, Dublin, Ireland). Plasma for this study was obtained from a subset of animals (as indicated in the figure legends). Blood was drawn and placed in sodium heparin tubes and centrifuged at 1,000*g* for 10 min and plasma aliquots were stored at –80°C until used. Animals were euthanized at the end of the study (day 45) or earlier if they became moribund due to radiation-induced sickness. Heart rate was monitored by auscultation at blood collection time points and at euthanasia. Gross pathological observations of body cavity and organs were recorded at the time of necropsy. The heart was excised and dissected into left and right ventricle and atrium, frozen immediately on dry ice and stored at –80°C until used.

Western Blot Analysis

Cytosolic and membrane proteins extracted from left ventricles using MEM-PER™ Plus membrane protein extraction kit and quantified using Pierce™ BCA protein assay kit. Equal amounts of denatured proteins were separated using 4–12% gradient polyacrylamide gels and transferred onto PVDF membrane. Blocking and incubation with primary and secondary antibodies were performed using WesternBreeze® Chemiluminescent kit (all reagents from Thermo Fisher Scientific™ Inc., Waltham, MA). Antibodies used were: p67-phox, ERK, eNOS and Na^+/K^+-ATPase (all from Santa Cruz Biotechnology® Inc., Dallas, TX); Superoxide Dismutase (SOD; Abcam®, Cambridge, MA); Akt, p-Akt, IGF-1R, p-IGF-1R, GAPDH (all from Cell Signaling Technology® Inc., Danvers, MA); and p-ERK and p-eNOS (both from R&D Systems™, Minneapolis, MN). Densitometric analysis of proteins was performed using Image Lab™ software version 5.2.1 (Bio-Rad® Laboratories Inc., Hercules, CA). GAPDH and Na^+/K^+-ATPase were used as the loading control for cytosolic and membrane fractions, respectively.

ELISA

Previously frozen plasma samples were thawed on ice, clarified by centrifugation at 10,000*g* for 30 min at 4°C, and plasma samples were diluted 1:100 times to measure the concentration of IGF-1 (Biomatik USA LLC, Wilmington, DE), 1:2,000 dilution to measure CRP (GenWay Biotech Inc., San Diego, CA), and 1:20 dilution to quantify BH4 (EIAab®, Wuhan, China). Undiluted plasma samples (50 µl) were used for quantification of endothelin-1 using a species-specific ELISA Kit (Cloud-Clone Corp., Katy, TX).

Nitric Oxide Measurement

Total nitric oxide concentrations were determined by enzymatic conversion of nitrate to nitrite. Plasma samples were filtered using 10 kDa filters (EMD Millipore, St. Charles, MO). Total nitrite concentration in 1:1 diluted plasma samples were measured using total nitric oxide and Nitrate/Nitrite assay kit according to manufacturer's instructions (R&D Systems).

Statistical Analysis

Statistical analyses were performed using SPSS® Statistics for Windows software version 24.0 (IBM® SPSS, Armonk, NY). Student's *t* test and Mann-Whitney U test were used to compare differences between groups in means or medians, according to data distribution. Student's paired *t* test and the Wilcoxon signed-rank test were used to compare preirradiation to euthanasia within groups. Survival time was compared using the log-rank test, and receiver operating characteristic (ROC) curves were used to describe how well the IGF-1-to-CRP ratio at euthanasia predicted survival and hemorrhage in the heart.

RESULTS

Radiation Sensitivity is not Associated with IGF-1 Levels

We established a dose-response relationship for GMP and SMP that received TBI with ^{60}Co gamma photons and medical management, as described in the Material and Methods, to determine the radiosensitivity in these two minipig strains. Table 1 shows the survival rate per TBI dose. Doses that were highly lethal for the GMP (2.1 and 2.3 Gy) were not lethal for the SMP (Table 1). Animals displayed signs of morbidity starting at day 14 postirradiation, as shown by nadir in platelet and neutrophil counts, reduced activity, petechiae, fever and frank bleeding. All the animals that received 1.7 Gy TBI survived until day 45. Moribund animals were euthanized at days 19, 23 and 29 (1.9 Gy); 17, 18, 21, 23, 25, 33 (2.1 Gy); and 14, 15, 15, 15, 16, 18, 18, 20, 27 (2.3 Gy). Decedents were characterized by multi-organ hemorrhages and faster heart rate at

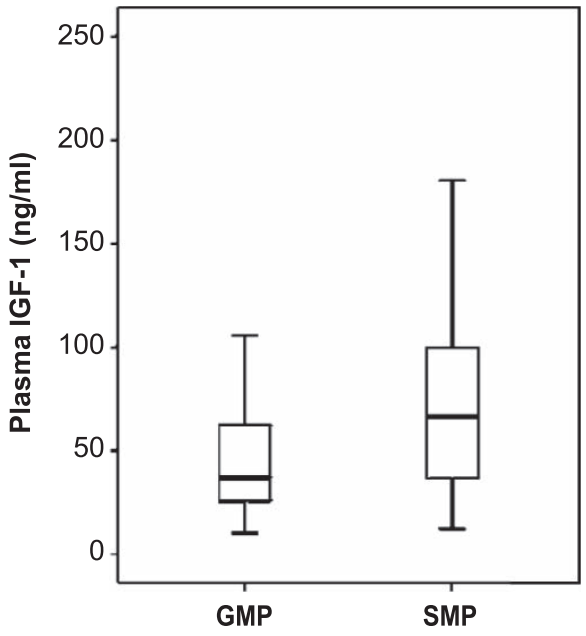

FIG. 1. IGF-1 levels. Plasma IGF-1 concentrations in adult male GMP (n = 22) and SMP (n = 24) were quantified using ELISA. Basal IGF-1 levels before irradiation were marginally higher in SMP compared to GMP ($P > 0.043$; Mann-Whitney U test).

euthanasia compared to survivors [decedents (150 ± 25) vs. survivors (128 ± 29); $P = 0.006$]. Heart hemorrhages were observed in 69% of the animals and degeneration in 31%, while hemorrhages and degeneration were only observed sporadically among animals euthanized at the end of the observation period. In spite of the difference in prevalence of hemorrhages, all minipigs, with the exception of one, became thrombocytopenic ($<50 \times 10^3/\mu l$) regardless of survival: the nadir for platelets among the decedents was 2.4 ± 1.3 × $10^3/\mu l$, whereas among the survivors it was 10.8 ± 1.3 × $10^3/\mu l$ ($P < 0.01$). The difference in platelet levels, although significant, did not convincingly explain the striking difference in hemorrhage prevalence observed between the two groups. Indeed, upon histological analysis at the completion of the 45-day observation period, heart hemorrhages were absent in 95% of the survivors, despite the fact that platelet counts remained below the $10 \times 10^3/\mu l$ cutoff for spontaneous bleeding (*37*) in 63% of the minipigs for an average of 14 ± 8 days (data not shown).

Next, we measured basal IGF-1 concentration in plasma in a subset of samples taken before irradiation (Fig. 1). The median IGF-1 value for the GMP was 37.0 ng/ml (minimum of 10.4; maximum of 105.7) and the SMP was 66.2 ng/ml (minimum of 12.3; maximum of 234.4). The IGF-1 levels were only marginally different between the two strains ($P = 0.043$, Mann-Whitney test). In contrast, the body weight of the GMP (10.3 ± 1.0 kg) was significantly smaller with respect to the SMP (15.5 ± 1.1 kg; $P < 0.001$), suggesting that in GMP the IGF-1 signaling was less efficient than in SMP.

IGF-1, CRP and Angiotensin II in the Irradiated Gottingen Minipig

IGF-1 promotes cardiovascular health through the production of NO and regulates anti-oxidant and anti-inflammatory mediators. Because of the tissue pathologies observed in the decedent animals, we investigated whether irradiation inhibited IGF-1 expression, downstream signaling cascades and regulators of IGF-1 activity. IGF levels were measured longitudinally in a total of 22 animals. Of these, 10 completed the 45-day observation period (survivors), and 12 were euthanized during the in-life phase of the study, due to radiation-induced injury (decedents). Manifest phase in these animals was characterized by decline in thrombocytes, granulocytes and erythrocytes; nadir was reached at approximately day 14–17 postirradiation and spontaneous recovery was observed in survivors starting from day 20–23 postirradiation; no recovery was observed in decedents. IGF-1 concentrations of individual animals, grouped by survival, are shown in Fig. 2A and B. Mean values of samples collected before irradiation and euthanasia, in animals stratified by survival outcome, are shown in Fig. 2C. Radiation-induced IGF-1 occurred early in all animals; however, the radiation response was much stronger in animals with unscheduled euthanasia. Furthermore, these animals showed a significant additional induction of IGF-1 starting at the manifest phase of the radiation sickness. Their IGF-1 levels at euthanasia were significantly higher with respect to preirradiation levels and to survivor animals ($P < 0.01$). A dose-dependent effect was not observed.

Next, we determined the relationship between IGF-1 and its negative regulators, CRP and angiotensin (Fig. 3). Both biomarkers were measured longitudinally from plasma samples of each individual animals. Representative examples of a survivor and decedent animal, are shown in Fig. 3A and B, respectively. In the survivor animal, the dynamic changes in CRP levels mirrored those of IGF-1. However, in the lethally irradiated animal, the equilibrium between IGF-1 and CRP was lost once the animals became sick, and IGF-1 levels increased regardless of CRP expression (Fig. 3B). Due to the high variability measured among individual animals for CRP and IGF-1, the reciprocal feedback between CRP and IGF-1 was quantified as the ratio of IGF-1 to CRP, normalized for each animal to its preirradiation values. IGF-1 to CRP ratio was significantly increased at euthanasia in decedent animals compared to preirradiation levels ($P = 0.007$; Fig. 3C). We next calculated the ratio of IGF-1 to CRP in n = 10 survivors and n = 12 decedents (Fig. 3D and E). The fold change in the ratio of IGF-1 to CRP from individual animals was increased rapidly after day 10 postirradiation in decedent animals compared to survivors. The average of the ratio at euthanasia was calculated for animals stratified by either survival or presence of heart hemorrhage. Values were significantly higher for those animals with hemorrhages in the heart (n = 9) with respect to those without hemorrhage

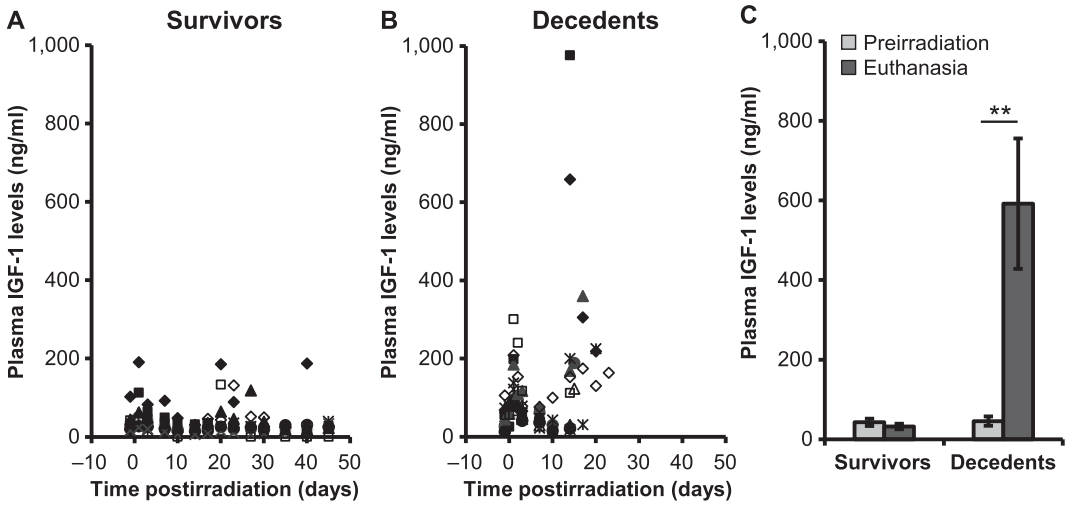

FIG. 2. Plasma IGF-1 levels increased in decedent GMP. IGF-1 levels were quantified longitudinally in survivors (n = 10) and decedents (n = 12) using ELISA (panels A and B). Values in scatter plots are IGF-1 levels from individual animals; each symbol represents an individual animal. Average IGF-1 levels are compared between preirradiation and euthanasia in survivors (n = 15) and decedents (n = 17) (panel C). IGF-1 was significantly increased in decedent animals at euthanasia compared to their preirradiation levels (**$P < 0.01$, Student's paired t test, two tails). Values plotted in panel C are mean ± SEM.

(n = 13, $P = 0.03$), as well as for decedents (n = 12) with respect to survivors (n = 10, $P = 0.03$; Fig. 3F). Angiotensin production, on the other hand, did not appear to be dramatically affected by radiation (Fig. 3G–I).

To confirm the changes in IGF-1 and CRP observed longitudinally overtime, we analyzed additional samples taken at euthanasia (Table 2). Mean IGF-1-to-CRP ratio was compared between survivors and decedents as well as between animals with and without heart hemorrhages; ROC curves were used to describe how well the IGF-1-to-CRP ratio predicted survival and hemorrhage. The area under the ROC curve exceeded 0.80 for mortality (0.837, CI 0.721–0.954) and for heart hemorrhages (0.808, CI 0.675–0.941), indicating that IGF-1 to CRP ratio was a good predictor for both mortality and heart hemorrhage (Supplementary Fig. S1; http://dx.doi.org/10.1667/RR14993.1.S1).

IGF-1 Downstream Signaling Pathways Shifted towards Pro-oxidant Environment in the Heart

Loss of regulatory feedback between IGF-1 and CRP suggested that IGF-1 lost a part of its downstream signaling, and prompted us to investigate the IGF-1 receptor (IGF-1R), components of both the IRS/PI3K/Akt/eNOS and Grb/Shc/MAPK/ET pathways and enzymes involved in the regulation of the redox system. Expression of IGF-1R was increased among decedent animals ($P < 0.01$), whereas its activity (p-IGF-1R) was decreased by more than twofold ($P < 0.001$) compared to survivors (Fig. 4A and B). PI3/Akt activity was significantly reduced in decedents, as shown by an approximately twofold decrease in the phosphorylation of Akt compared to survivors ($P < 0.001$); total Akt levels remain unaffected (Fig. 4C and D). Less dramatic changes were observed in the activity of p44/42 MAP kinases with respect to Akt (Fig. 4E and F). Taken together, these findings suggest that the anti-inflammatory, anti-oxidant pathways were preferentially inhibited in decedent animals.

Next, we measured pro- and anti-oxidant enzyme expression. A greater-than-twofold increase in the expression of p67-phox, a regulatory subunit of NADPH oxidase 2 (NOX2), was observed in decedents compared to survivors ($P < 0.01$; Fig. 5A), whereas expression of SOD and catalase was only marginally decreased ($P < 0.05$). These observations indicate an imbalance between the pro-oxidant and anti-oxidant defense in the heart of decedent animals.

eNOS, BH4 and Vascular Dysfunction

eNOS is an enzyme essential for a healthy cardiovascular system due to its ability to produce NO. Functional catalysis of eNOS is contingent upon its ability to couple NADPH oxidation with NO synthesis, for which the redox-sensitive cofactor BH4 plays a crucial role. The antithetic ability of eNOS to produce either NO or superoxide depending on the bioavailability of BH4, and the shift towards a pro-oxidant milieu in the decedent animals, prompted us to evaluate eNOS expression and activity in the heart of irradiated minipig, as well as plasma concentration of BH4, NO and ET-1. Both eNOS and phospho-eNOS were increased in decedents compared to survivors, however, the increase in the p-eNOS expression was not statistically significant (Fig. 6). BH4 levels decreased in decedents over time at a faster rate compared to survivors (Fig. 7A and B). Analysis of BH4 comparing euthanasia with preirradiation values revealed a greater-than-twofold drop ($P < 0.01$; Fig. 7C). Similarly, over time, assessment of total nitrite as an index of NO indicated that levels increased shortly after irradiation but eventually declined significantly when the

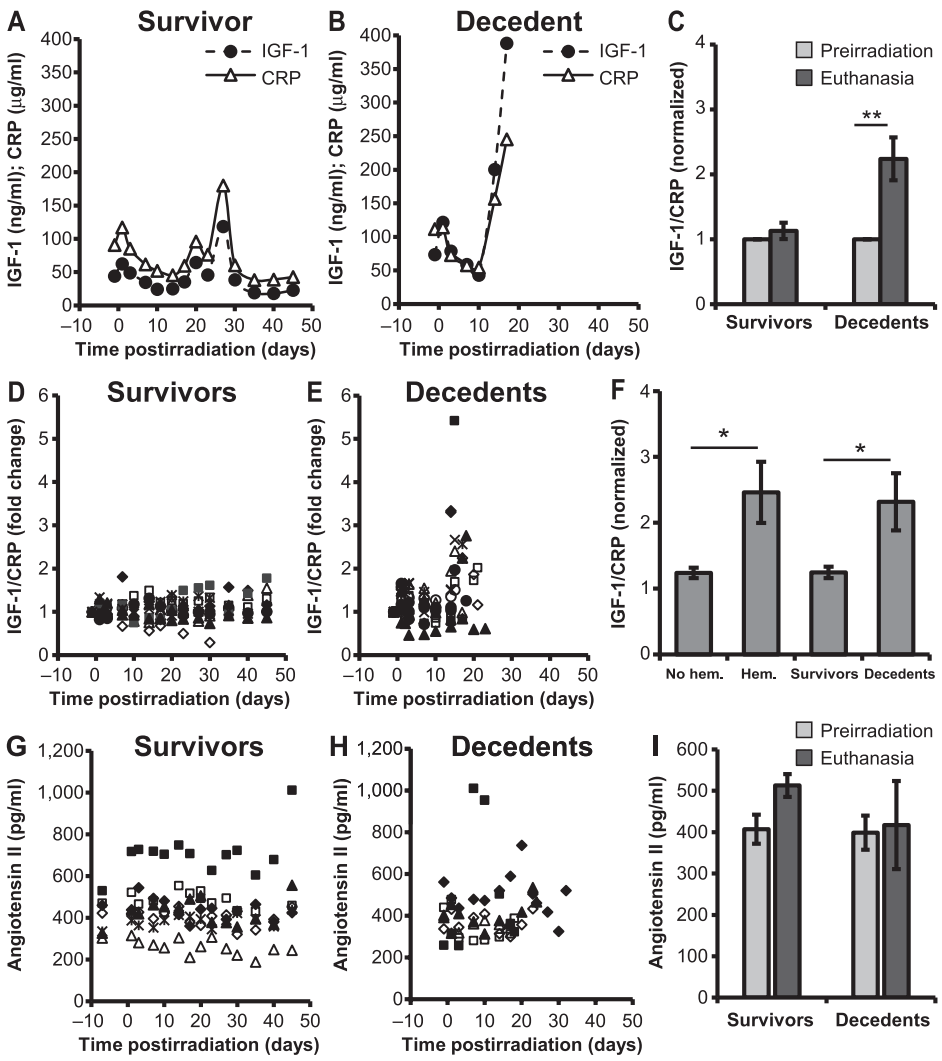

FIG. 3. Dynamic changes in the expression of IGF-1 and CRP. Plasma IGF-1 and CRP levels were compared longitudinally in survivors and decedents (panels A, B, D and E). Representative IGF-1 and CRP levels from one survivor and one decedent (panels A and B, respectively) show that the expression of IGF-1 paralleled that of CRP, however, the equilibrium was lost when the animals became sick due to radiation injury (panel B). Fold changes in the IGF-1-to-CRP ratio were higher at euthanasia than preirradiation in decedents (panel C). IGF-1 and CRP expression levels from individual animals were normalized to their preirradiation levels and are shown as the relative fold changes for survivors (panel D) and decedents (panel E). Panel F: The ratio of CRP to IGF-1 in animals with and without hemorrhages (hem) in heart and also decedents compared to survivors. Values plotted in panels C and F are mean average ratios after normalization. Panels G–I: Plasma angiotensin II concentration from individual survivors (panel G), decedents (panel H) and average angiotensin II levels at preirradiation and at euthanasia (panel I). There were no statistically significant differences in the concentration of angiotensin II in decedents compared to survivors. Values plotted in panels C, F and I are mean ± SEM. Data analyzed using Student's paired *t* test; n = 10–12/group. $*P < 0.05$; $**P < 0.01$. Each symbol in panels D, E, G and H represent an individual animal.

TABLE 2
IGF-1-to-CRP Ratio at Euthanasia in Gottingen Minipigs after TBI

Groups	No. of animals	Mean ± SD	Median
Decedents*	17	1.98 ± 1.057	1.69
Survivors	23	1.17 ± 0.343	1.13
Heart hemorrhage present	15	2.02 ± 1.086	1.69
Heart hemorrhage absent	25	1.21 ± 0.423	1.16

* One animal was found dead; plasma sample was not available for analysis.

animals became sick and moribund (Fig. 7D–E). Nitrite concentration at euthanasia was dramatically decreased with respect to preirradiation values ($P < 0.001$; Fig. 7F). These observations indicate a potential role played by BH4 and NO in radiation-induced lethality. Unlike BH4 and NO, ET-1 levels were not significantly different between survivors and decedents and did not decline at euthanasia (Fig. 7G–I). However, the ratio between ET-1 to BH4, as well as ET-1 to NO, was significantly increased in the decedent animals, indicating a strong imbalance in the regulation of vascular

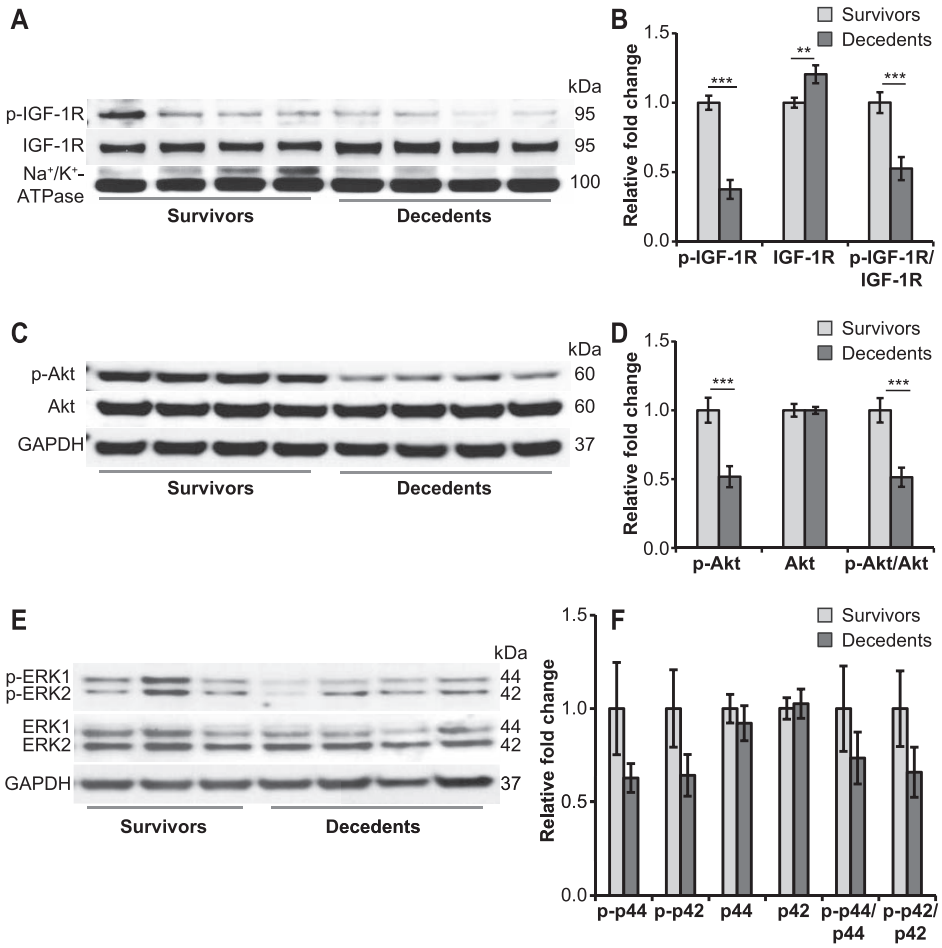

FIG. 4. Deregulated IGF-1R signaling in decedents. Immunoblots were performed using antibodies against p-IGF-1R, IGF-1R, Akt, p-Akt, p-ERK1/2 and ERK1/2 (panels A, C and E; n = 7–12/group). Shown here are representative images. Protein bands were quantified using densitometry measurements (panels B, D and F). Expression of p-IGF-1R was significantly reduced in decedents, whereas total IGF-1R was increased in the heart (panels A and B). p-Akt levels were also decreased, however, the expression of total Akt remains unchanged (panels C and D). Differences were observed in the expression of total ERK1/2 and p-ERK-1/2 but they were not statistically significant (panels E and F). Na^+/K^+-ATPase (membrane) or GAPDH (cytosolic) was used as the loading control. Values plotted are mean relative fold change ± SEM. Student's *t* test was used for comparison of survivors vs. decedents. $^{**}P < 0.01$; $^{***}P < 0.001$.

tone and a shift towards vasoconstriction (Fig. 8A–F). The large standard deviation in Fig. 8F reflects two extremely high values of the ET-1-to-NO ratio that fall outside the range reported in the scatter plot.

DISCUSSION

The Gottingen minipig is a sensitive model of radiation injury, characterized by occurrence of hemorrhages at relatively low radiation doses. The GH/IGF-1 pathway plays a critical role in the maintenance of cardiovascular health and growth, and has been shown to elicit beneficial responses against the effects of radiation injury (*24*). Here we sought to determine if GH/IGF-1 was expressed at lower levels in the GMP with respect to the SMP, a breed with a growth curve steeper than that observed for the GMP and less sensitive to radiation [(*2*) and our data]. In addition, we investigated the IGF-1 downstream signaling pathways PI3K/Akt/eNOS and MAPK/ET-1, the negative regulators of IGF-1 cardiovascular-protective function (CRP and angiotensin), pro- and anti-oxidant enzymes, as well as markers of endothelial dysfunction, with the goal of elucidating the mechanisms leading to radiation-induced vascular damage observed at hematopoietic acute radiation syndrome (H-ARS) doses in the GMP model.

Under identical conditions, TBI doses sufficient to cause high lethality (70%) in the GMP had no effect on the survival of the SMP, confirming the relative radiosensitivity of the GMP compared to the SMP. IGF-1 expression levels between the two breeds were barely different, despite the large difference in body size. These findings were surprising, suggesting that the efficiency of the IGF-1

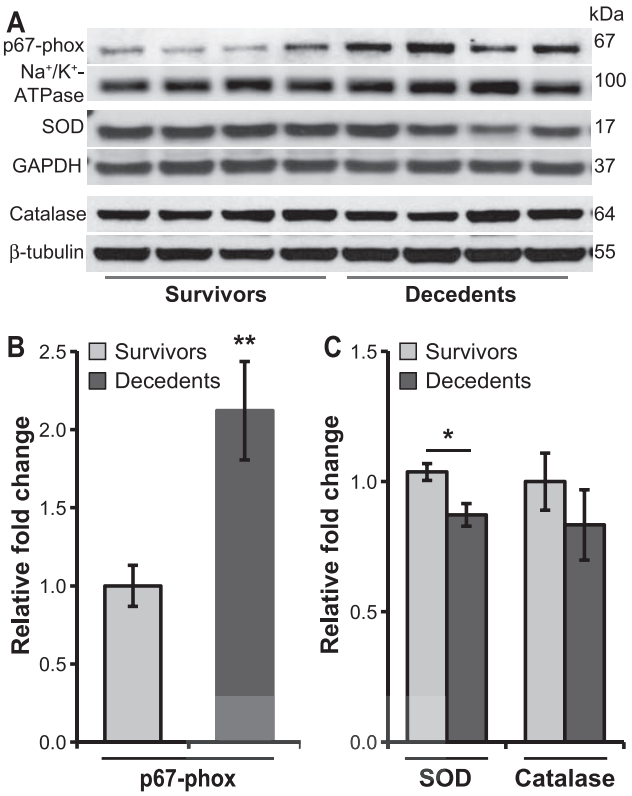

FIG. 5. Increased oxidative stress in decedents. Immunoblots were performed using α-p67-phox, α-SOD1 and α-catalase antibody and were normalized to Na^+/K^+-ATPase, GAPDH and β-tubulin, respectively. NADPH oxidase subunit, p67-phox expression was increased in decedents. The expression of superoxide dismutase (SOD) was decreased, whereas the catalase levels were not altered in decedents compared to survivors (panel A). Protein bands were quantified using densitometry (panels B and C). Values plotted are mean relative fold changes ± SEM; Student's *t* test was used for comparison of survivors vs. decedents. n = 8–11/group.*$P < 0.05$; **$P < 0.01$.

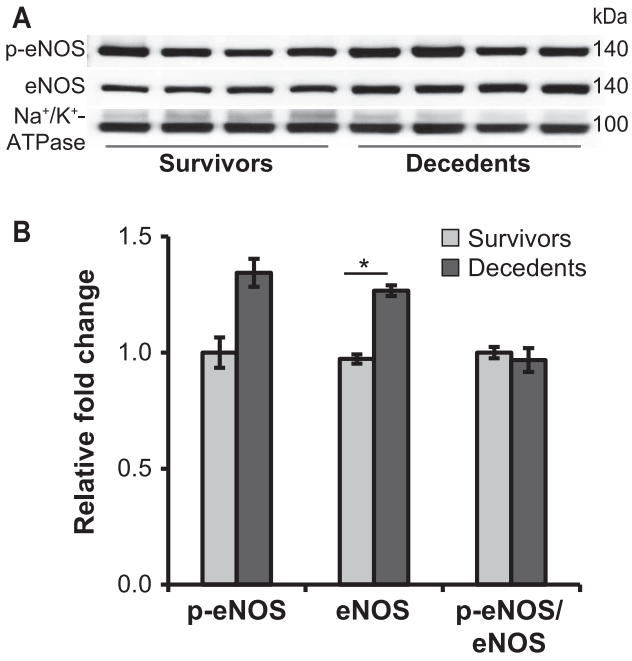

FIG. 6. Altered expression and the activity of eNOS in decedents. Panel A: Representative Western blots show the expression of eNOS in the heart membrane fractions of survivors and decedents. Immunoblots were performed using antibodies against eNOS and p-eNOS (S1177) and were normalized to Na^+/K^+-ATPase. Panel B: Densitometric analysis of p-eNOS, total eNOS and the ratio of p-eNOS to eNOS. The expression of total p-eNOS and eNOS was increased in decedents, however, the increase in p-eNOS was not statistically significant. All data are expressed as mean relative fold changes ± SEM; n = 10–13/group. Student's *t* test was used for comparison of survivors vs. decedents. *$P < 0.05$.

pathway in the GMP might be lower with respect to other strains and may require higher concentrations of the ligand. Evidence supporting an unusual GH/IGF-1 axis in the Gottingen with respect to other minipig strains has been reported in studies performed by others. In a study by Johansen *et al.* (*19*), the lack of GH secretion after intravenous glucose tolerance testing and high-fat/high-energy feeding in the obese GMP was attributed to a possibly unusual GH/IGF-1 axis. Similarly, a study on the effect of somatostatin, a GH-inhibiting factor, and GH secretion in minipigs of different body size, suggested that GH was significantly higher at baseline in the larger German Landrace minipig with respect to the small GMP (age matched, 6–8 months old), and that the response to growth hormone-releasing factor and somatostatin were significantly different between the two breeds, suggesting significant differences in the control of GH release (*38, 39*).

We next assessed variation in the blood levels of IGF-1 after irradiation in the GMP. IGF-1 was expected to confer some protection from radiation and to be associated with survival, as evidenced in mouse studies (*25–28*) and by the use of IGF-1 inhibitors to sensitize cancer cells to radiation therapy (*24*). As expected, we found that IGF-1 was induced by radiation; however, elevated IGF-1 levels were found to be positively associated with lack of survival and heart hemorrhages, suggesting that radiation might alter downstream signaling of IGF-1. An association between decreased NO signaling and bleeding has been demonstrated in the brain of a mouse model of experimental malaria, where administration of NO donors restored NO signaling and reduced vascular leakage and petechiae (*40*). We therefore measured downstream targets of IGF-1 involved in the regulation of NO synthesis as well as CRP and angiotensin, to evaluate if radiation inhibited NO production and caused a disturbance in the NO and ET-1 balance.

IGF-1 and CRP, but not angiotensin II, were consistently and significantly induced in decedent animals with respect to preirradiation levels. Receiver operating characteristic (ROC) curves were used to describe how well the IGF-1 to CRP ratio at euthanasia predicted survival and hemorrhage in the heart. The area under the ROC curve exceeded 0.80 for both cases, indicating good prediction and pointing to an important role for the loss of equilibrium between IGF-1 and CRP in the development of radiation injury. In surviving animals, IGF-1 exhibited an exquisite cross-

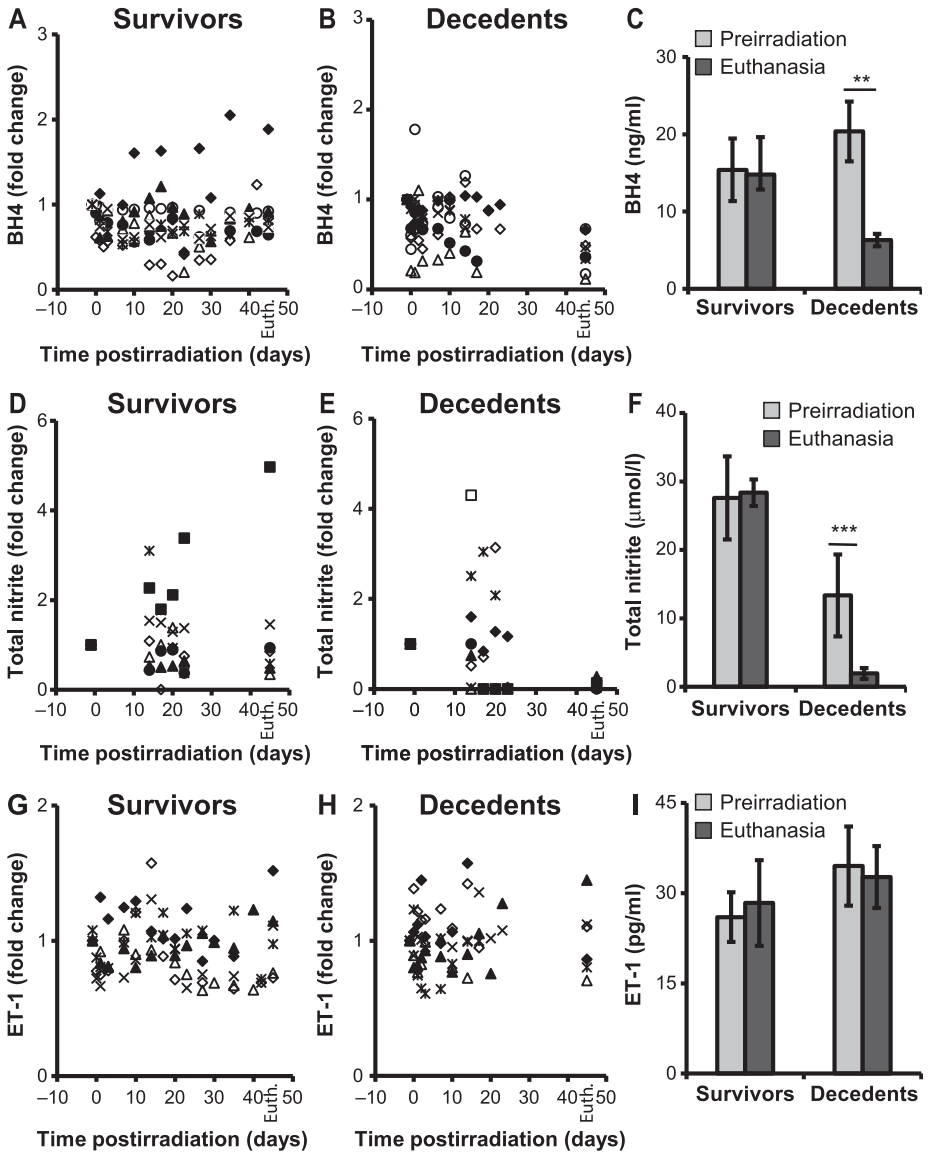

FIG. 7. BH4, NO and ET-1 levels were altered in decedents. Plasma BH4, NO and ET-1 concentrations were measured longitudinally in survivors and decedents from preirradiation through necropsy. Significant reduction in the production of BH4 (panels A and B) as well as NO (panels D and E) was evident in decedents compared to survivors. The concentration of BH4 and NO at preirradiation vs. euthanasia are shown in panels C and F, respectively. Plasma ET-1 levels from individual survivors (panel G) and decedents (panel H) and average ET-1 levels at preirradiation and at euthanasia (panel I). There was no statistically significant difference in the concentration of ET-1 in decedents compared to survivors (panel I). Values shown at day 45 in survivors (panels A, D and G) and decedents (panels B, E and H) are BH4, total nitrite and ET-1 levels at euthanasia (Euth). Student's paired *t* test was used for comparison of preirradiation to euthanasia. n = 8/group. $*P < 0.01$; $**P < 0.001$. BH4 = tetrahydrobiopterin; NO = nitric oxide; ET-1 = endothelin-1.

regulation with CRP, whereas the equilibrium between IGF-1 and CRP was lost in decedents. In this group, IGF-1 levels increased regardless of CRP expression, suggesting potential onset of IGF-1 resistance. Our data confirmed that the IGF-1/PI3K/Akt pathway was inhibited in GMP decedent animals, while the MAPK pathway remained active. Analysis of SMP plasma and heart tissue lysates showed similar inhibition of the IGF-1/PI3/Akt pathway in decedents compared to survivors (data not shown). This situation was suggestive of selective insulin/IGF-1 resistance, where the MAPK/ET-1 pathway prevailed over the PI3K/Akt pathway and mediated inflammation and vascular dysfunction. Indeed, we showed that the ratios between ET-1 and BH4 as well as ET-1 and NO were enhanced dramatically among decedent animals. In addition, these animals had increased levels of CRP and p67-phox, a subunit of NOX2. p67-phox is necessary for NOX2 activation and production of superoxide [reviewed in (*41*)]. In a published clinical study of chronic heart failure,

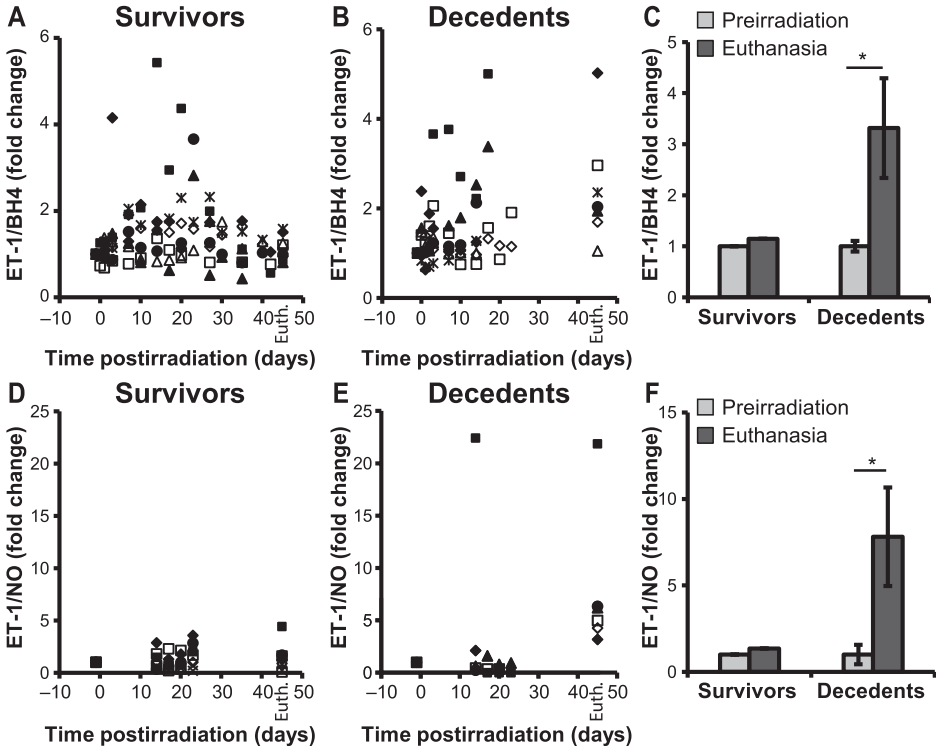

FIG. 8. Increased ratios of ET-1 to BH4 and ET-1 to nitric oxide. Fold changes in the ratios of individual animals in the expression of ET-1 to BH4 (panels A and B) and ET-1 to NO (panels D and E). Each symbol represents an individual animal. Average ratios of ET-1 to BH4 (panel C) and ET-1 to NO (panel F) were increased at euthanasia compared to their preirradiation levels. n = 6-8; Wilcoxon signed rank test, $*P < 0.05$. BH4 = tetrahydrobiopterin; NO = nitric oxide; ET-1 = endothelin-1.

upregulation of CRP was shown to be associated with increased expression of p67-phox (*41*).

Induction and phosphorylation of eNOS in spite of Akt inactivation was not surprising. Thrombin and histamine have been shown to phosphorylate eNOS on Ser-1177 through AMPK and independent of PI3K/Akt, under oxidative stress conditions (*42–46*). Therefore, induction of eNOS expression and phosphorylation were expected to occur under oxidative stress independent of Akt activity. However, in the pro-inflammatory and pro-oxidative milieu described above for the decedent animals, activation of eNOS may cause severe harm. The production of NO requires eNOS to be properly coupled through the action of BH4. Under conditions of oxidative stress, BH4 is oxidized to BH2, causing eNOS to uncouple and to produce superoxide instead of NO, altering the NO/ET-1 equilibrium and promoting vascular dysfunction (*47, 48*). CRP can also uncouple eNOS, directly or through induction of NADPH oxidase and reactive oxygen species (ROS) production (*49, 50*). Our data suggest that decline in BH4 levels and increase in inflammatory and pro-oxidant mediators induced eNOS uncoupling and further increased oxidative stress at the expense of NO production. As a consequence, decedent animals were characterized by a significant drop in NO levels and extensive vascular damage.

CONCLUSIONS AND LIMITATIONS

In conclusion, we suggest that onset of selective IGF-1 resistance may play a critical role in the etiology of the H-ARS. According to this paradigm, radiation-induced selective IGF-1 resistance is associated with inhibition of the anti-inflammatory anti-oxidative stress PI3K/Akt pathway, whereas the pro-inflammatory MAPK kinase pathway remains at least partially functional. The pro-oxidant, pro-inflammatory environment favors oxidative stress, uncoupling of eNOS, imbalance between NO and ET-1, onset of endothelial dysfunction and development of pro-inflammatory, pro-thrombotic endothelial features, furthering a vicious cycle that amplifies ROS-induced damage which, in the presence of thrombocytopenia, can lead to bleeding. Indeed, factors other than low platelet counts are necessary to provoke bleeding, as demonstrated by a study on models of localized dermatitis, stroke and lung inflammation in thrombocytopenic mice (*51*). In these models, massive hemorrhage occurred only in the area of inflammation and was not observed mice that had no inflammation, in spite of their thrombocytopenic status.

We also propose that the radiosensitivity of the GMP may be due to innately low IGF-1 activity, which was selected through genetic drifting to ensure the small size of the breed (*5, 52*), and to a predisposition to develop endothelial

dysfunction (*53*). In the human population, IGF-1 levels are found to be decreased among the elderly, and both high and low concentration of IGF-1 are at the center of several pathological conditions including cardio-metabolic syndrome, diabetes, atherosclerosis, burn and wound injury, systemic inflammatory response syndrome, neurodegeneration and Alzheimer's disease (*54–59*). For these cases, a relatively small dose of environmental stressors might be sufficient to further alter downstream signaling of the IGF-1 pathway, triggering selective resistance and promoting self-perpetuating oxidative stress, inflammation and vascular damage while inhibiting production of NO. Further characterization of the insulin/IGF-1 pathway as a target for countermeasure development, biomarker discovery and relationship with survival and co-morbidities is warranted. The value of the current work is limited by the use of a single animal model. If confirmed in multiple animal species, our findings may have important implications for the etiology and treatment of ARS.

SUPPLEMENTARY INFORMATION

Fig. S1. ROC curves for IGF to CRP ratio as a predictor of heart hemorrhages and mortality.

ACKNOWLEDGMENTS

This work was supported by funding from National Institute of Allergy and Infectious Diseases OD-0505-01, BARDA IAA750114PR970036. Special thanks to the AFRRI Cobalt facility and the Veterinary Sciences Department staff for their dedication to the project and superb animal care. The opinions or assertions contained herein are the private views of the authors and are not necessarily those of the Armed Forces Radiobiology Research Institute (AFRRI), the Uniformed Services University of the Health Sciences or the Department of Defense. The funding agencies had no role in study design, data collection and analysis, decision to publish or preparation of the manuscript.

Received: November 27, 2017; accepted: April 23, 2018; published online: May 29, 2018

REFERENCES

1. Moroni M, Lombardini E, Salber R, Kazemzedeh M, Nagy V, Olsen C, et al. Hematological changes as prognostic indicators of survival: similarities between Gottingen minipigs, humans, and other large animal models. PLoS One 2011; 6:e25210.
2. Mandel L, Travnícek J, Talafantova M, Zahradníckova M. The LD50/30 and the survival time in whole-body gamma-irradiated conventional and germfree Minnesota miniature piglets. Z Versuchstierkd 1980; 22:96–100.
3. Krigsfeld GS, Shah JB, Sanzari JK, Lin L, Kennedy AR. Evidence of disseminated intravascular coagulation in a porcine model following radiation exposure. Life Sci Space Res (Amst) 2014; 3:1–9.
4. Moroni M, Coolbaugh TV, Lombardini E, Mitchell JM, Moccia KD, Shelton LJ, et al. Hematopoietic radiation syndrome in the Gottingen minipig. Radiat Res 2011; 176:89–101.
5. Simianer H, Kohn F. Genetic management of the Göttingen minipig population. J Pharmacol Toxicol Methods 2010; 62:221–6.
6. DeBosch BJ. Muslin AJ. Insulin signaling pathways and cardiac growth. J Mol Cell Cardiol 2008; 44:855–64.
7. Muniyappa R, Montagnani M, Koh KK, Quon MJ. Cardiovascular actions of insulin. Endocr Rev 2007; 28:463–91.
8. Aguirre GA, De Ita JR, de la Garza RG, Castilla-Cortazar I. Insulin-like growth factor-1 deficiency and metabolic syndrome. J Transl Med 2016; 14:3.
9. Bajpai A, Menon PS. Insulin like growth factors axis and growth disorders. Indian J Pediatr 2006; 73:67–71.
10. King GL, Park K, Li Q. Selective insulin resistance and the development of cardiovascular diseases in diabetes: The 2015 Edwin Bierman Award Lecture. Diabetes 2016; 65:1462–71.
11. Hink U, Li H, Mollnau H, Oelze M, Matheis E, Hartmann M, et al. Mechanisms underlying endothelial dysfunction in diabetes mellitus. Circ Res 2001; 88:E14–22.
12. Zhao Y, Vanhoutte PM, Leung SW. Vascular nitric oxide: Beyond eNOS. J Pharmacol Sci 2015; 129:83–94.
13. Napoli C. de Nigris F, Williams-Ignarro S, Pignalosa O, Sica V, Ignarro LJ. Nitric oxide and atherosclerosis: an update. Nitric Oxide 2006; 15:265–79.
14. Roberts RE. The extracellular signal-regulated kinase (ERK) pathway: a potential therapeutic target in hypertension. J Exp Pharmacol 2012; 4:77–83.
15. Hage FG. C-reactive protein and hypertension. J Hum Hypertens 2014; 28:410–5.
16. Venugopal SK, Devaraj S, Yuhanna I, Shaul P, Jialal I. Demonstration that C-reactive protein decreases eNOS expression and bioactivity in human aortic endothelial cells. Circulation 2002; 106:1439–41.
17. Verma S, Kuliszewski MA, Li SH, Szmitko PE, Zucco L, Wang CH, et al. C-reactive protein attenuates endothelial progenitor cell survival, differentiation, and function: further evidence of a mechanistic link between C-reactive protein and cardiovascular disease. Circulation 2004; 109:2058–67.
18. Hein TW, Singh U, Vasquez-Vivar J, Devaraj S, Kuo L, Jialal I. Human C-reactive protein induces endothelial dysfunction and uncoupling of eNOS in vivo. Atherosclerosis 2009; 206:61–8.
19. Devaraj S, Kumaresan PR, Jialal I. C-reactive protein induces release of both endothelial microparticles and circulating endothelial cells in vitro and in vivo: further evidence of endothelial dysfunction. Clin Chem 2011; 57:1757–61.
20. Tanigaki K1, Mineo C, Yuhanna IS, Chambliss KL, Quon MJ, Bonvini E, et al. C-reactive protein inhibits insulin activation of endothelial nitric oxide synthase via the immunoreceptor tyrosine-based inhibition motif of FcgammaRIIB and SHIP-1. Circ Res 2009; 104:1275–82.
21. Järvisalo MJ, Harmoinen A, Hakanen M, Paakkunainen U, Viikari J, Hartiala J, et al. Elevated serum C-reactive protein levels and early arterial changes in healthy children. Arterioscler Thromb Vasc Biol 2002; 22:1323–8.
22. Fichtlscherer S, Breuer S, Schachinger V, Dimmeler S, Zeiher AM. C-reactive protein levels determine systemic nitric oxide bioavailability in patients with coronary artery disease. Eur Heart J 2004; 25:1412–8.
23. Nguyen Dinh Cat A, Montezano AC, Burger D, Touyz RM. Angiotensin II, NADPH oxidase, and redox signaling in the vasculature. Antioxid Redox Signal 2013; 19:1110–20.
24. Valenciano A, Henriquez-Hernandez LA, Moreno M, Lloret M, Lara PC. Role of IGF-1 receptor in radiation response. Transl Oncol 2012; 5:1–9.
25. Zhou D, Deoliveira D, Kang Y, Choi SS, Li Z, Chao NJ, et al. Insulin-like growth factor 1 mitigates hematopoietic toxicity after lethal total body irradiation. Int J Radiat Oncol Biol Phys 2013; 85:1141–8.
26. Van Landeghem L, Santoro MA, Mah AT, Krebs AE, Dehmer JJ,

McNaughton KK1, et al. IGF1 stimulates crypt expansion via differential activation of 2 intestinal stem cell populations. FASEB J 2015; 29:2828–42.

27. Qiu W, Leibowitz B, Zhang L, Yu J. Growth factors protect intestinal stem cells from radiation-induced apoptosis by suppressing PUMA through the PI3K/AKT/p53 axis. Oncogene 2010; 29:1622–32.

28. Michaylira CZ, Simmons JG, Ramocki NM, Scull BP, McNaughton KK, Fuller CR, et al. Suppressor of cytokine signaling-2 limits intestinal growth and enterotrophic actions of IGF-I in vivo. Am J Physiol Gastrointest Liver Physiol 2006; 291:G472–81.

29. Suman S, Kallakury BV, Fornace AJ Jr, Datta K. Protracted upregulation of leptin and IGF1 is associated with activation of PI3K/Akt and JAK2 pathway in mouse intestine after ionizing radiation exposure. Int J Biol Sci 2015; 11:274–83.

30. Floratou K, Giannopoulou E, Antonacopoulou A, Karakantza M, Adonakis G, Kardamakis D, et al. Oxidative stress due to radiation in CD34(+) hematopoietic progenitor cells: protection by IGF-1. J Radiat Res 2012; 53:672–85.

31. Liu SJ, Zhong Y, You XY, Liu WH, Li AQ, Liu SM. Insulin-like growth factor 1 opposes the effects of C-reactive protein on endothelial cell activation. Mol Cell Biochem 2014; 385:199–205.

32. Azimzadeh O, Sievert W, Sarioglu H, Merl-Pham J, Yentrapalli R, Bakshi MV, et al. Integrative proteomics and targeted transcriptomics analyses in cardiac endothelial cells unravel mechanisms of long-term radiation-induced vascular dysfunction. J Proteome Res 2015; 14:1203–19.

33. Elliott TB, Deutz NE, Gulani J, Koch A, Olsen CH, Christensen C, et al. Gastrointestinal acute radiation syndrome in Gottingen minipigs (Sus Scrofa Domestica). Comp Med 2014; 64:456–63.

34. Moroni M, Ngudiankama BF, Christensen C, Olsen CH, Owens R, Lombardini ED, et al. The Gottingen minipig is a model of the hematopoietic acute radiation syndrome: G-CSF stimulates hematopoiesis and enhances survival from lethal total-body gamma-irradiation. Int J Radiat Oncol Biol Phys 2013; 86:986–92.

35. Kaur A, Vemalapally N, Severson G, Gulani J, Bolduc D, Moroni M. Development of a pediatric model of hematopoietic acute radiation syndrome (H-ARS) and countermeasure testing using the Gottingen minipigs. Rad Appl 2017; 2:75–81.

36. Levi M, van der Poll T. Coagulation and sepsis. Thromb Res 2017; 149:38–44.

37. Izak M, Bussel JB. Management of thrombocytopenia. F1000Prime Reports. 2014; 6:45.

38. Johansen T, Hansen HS, Richelsen B, Malmlöf R. The obese Gottingen minipig as a model of the metabolic syndrome: dietary effects on obesity, insulin sensitivity, and growth hormone profile. Comp Med 2001; 51:150–5.

39. Torronteras R, Gracia-Navarro F, Elsaesser F. Different effects of somatostatin on in vitro growth hormone release in two porcine breeds with different growth rates. J Neuroendocrinol 1996; 8:891–900.

40. Gramaglia I, Sobolewski P, Meays D, Contreras R, Nolan JP, Frangos JA, et al. Low nitric oxide bioavailability contributes to the genesis of experimental cerebral malaria. Nat Med 2006; 12:1417–22.

41. Schroder K, Weissmann N, Brandes RP. Organizers and activators: Nox proteins impacting vascular function. Free Rad Biol Med 2017; 109:22–32.

42. Cardaci S., Filomeni G., Ciriolo M.R. Redox implications of AMPK-mediated signal transduction beyond energetic clues. J Cell Sci 2012; 125:2115–25.

43. Thors B, Halldorsson H, Thorgeirsson G. Thrombin and histamine stimulate endothelial nitric-oxide synthase phosphorylation at Ser1177 via an AMPK mediated pathway independent of PI3K-Akt. FEBS Lett 2004; 573:175–80.

44. Motley ED, Eguchi K, Patterson MM, Palmer PD, Suzuki H, Eguchi S. Mechanism of endothelial nitric oxide synthase phosphorylation and activation by thrombin. Hypertension 2007; 49:577–83.

45. Jin SW, Choi CY, Hwang YP, Kim HG, Kim SJ, Chung YC, et al. Betulinic acid increases enos phosphorylation and no synthesis via the calcium-signaling pathway. J Agric Food Chem 2016; 64:785–91.

46. Zheng S, Li W, Xu M, Bai X, Zhou Z, Han J, et al. Calcitonin gene-related peptide promotes angiogenesis via AMP-activated protein kinase. Am J Physiol Cell Physiol 2010; 299:C1485–92.

47. Chen CA, Druhan LJ, Varadharaj S, Chen YR, Zweier JL. Phosphorylation of endothelial nitric-oxide synthase regulates superoxide generation from the enzyme. J Biol Chem 2008; 283:27038–47.

48. Fulton D, Gratton JP, McCabe TJ, Fontana J, Fujiot Y, Walsh K, et al. Regulation of endothelium-derived nitric oxide production by the protein kinase Akt. Nature 1999; 399:597–601.

49. Taylor-Fishwick DA. NOX, NOX Who is there? The contribution of NADPH oxidase one to beta cell dysfunction. Front Endocrinol (Lausanne) 2013; 4:40.

50. Qamirani E, Ren Y, Kuo L, Hein TW. C-reactive protein inhibits endothelium-dependent NO-mediated dilation in coronary arterioles by activating p38 kinase and NAD(P)H oxidase. Arterioscler Thromb Vasc Biol 2005; 25:995–1001.

51. Goerge T, Ho-Tin-Noe B, Carbo C, Benarafa C, Remold-O'Donnell E, Zhao BQ, et al. Inflammation induces hemorrhage in thrombocytopenia. Blood 2008; 111:4958–64.

52. Garke C, Ytournel F, Sharifi AR, Pimentel EC, Ludwig A, Simianer H. Footprints of recent selection and variability in breed composition in the Gottingen minipig genome. Anim Genet 2014; 45:381–91.

53. Jeppesen G, Skydsgaard M. Spontaneous background pathology in Gottingen minipigs. Toxicol Pathol 2015; 43:257–66.

54. Alberti KG, Zimmet P, Shaw J. The metabolic syndrome-a new worldwide definition. Lancet 2005; 366:1059–62.

55. van Bunderen CC, van Nieuwpoort IC, van Schoor NM, Deeg DJ, Lips P, Drent ML. The association of serum insulin-like growth factor-1 with mortality, cardiovascular disease, and cancer in the elderly: a population-based study. J Clin Endocrinol Metab 2015; 95:4616–24.

56. Westwood AJ, Beiser A, Decarli C, Harris TB, Chen TC, He XM, et al. Insulin-like growth factor-1 and risk of Alzheimer dementia and brain atrophy. Neurology 2014; 82:1613–19.

57. Zemva J, Schubert M. The role of neuronal insulin/insulin-like growth factor-1 signaling for the pathogenesis of Alzheimer's disease: possible therapeutic implications. CNS Neurol Disord Drug Targets 2014; 13:322–37.

58. Elijah I, Branski LK, Finnerty CF, Herndon DN. The GH/IGF-1 system in critical illness. Best Pract Res Clin Endocrinol Metab 2011; 25:759–67.

59. Blackstock CD, Higashi Y, Sukhanov S, Shai SY, Stefanovic B, Tabony AM, et al. Insulin-like growth factor-1 increases synthesis of collagen type I via induction of the mRNA-binding protein LARP6 expression and binding to the 5′ stem-loop of COL1a1 and COL1a2 mRNA. J Biol Chem 2014; 289:7264–74.